Agrociencia

HYDROLOGICAL MODEL WITH IMERG IMAGES OF THE COAHUAYANA RIVER BASIN, JALISCO, MEXICO

Pedro **Girón-Méndez**[1], Laura Alicia **Ibáñez-Castillo**[1*], Ramón **Arteaga-Ramírez**[1], Mario Alberto **Vázquez-Peña**[1]

[1] Universidad Autónoma Chapingo. Departamento de Irrigación, Posgrado en Ingeniería Agrícola y Uso Integral del Agua. Carretera México-Texcoco km 38.5, Chapingo, Texcoco, State of Mexico, Mexico. C. P. 56227.
* Author for correspondence: libacas@gmail.com

Citation: Girón-Méndez P, Ibáñez-Castillo LA, Arteaga-Ramírez R, Vázquez-Peña MA. 2023. Hydrological model with IMERG images of the Coahuayana River basin, Jalisco, Mexico. **Agrociencia** https://doi.org/ 10.47163/agrociencia.v57i2.2893

Editor in Chief:
Dr. Fernando C. Gómez Merino

Received: October 26, 2022.
Approved: February 07, 2023.
Published in Agrociencia: March 15, 2023.

ABSTRACT

Hydrologic modeling using precipitation estimated from satellite images considers temporal and spatial variability of the precipitation. The objective of this study was to model the rain-runoff process and calibrate some hourly hydrograms from the Coahuayana River Basin in Jalisco, Mexico. IMERG version 6 satellite rainfall images during the maximum events occurred in July 2010, October 2011, September 2013, October 2015, and August 2021 were used. The basin is located in the states of Jalisco, Colima, and Michoacán, and covers an area of 7332 km^2. The hydrologic model was developed using the program HEC-HMS and calibrated at the CONAGUA hydrometric station Callejones. The methods used for the calculations are the runoff curve number and Clark's modified unitary hydrogram. The results obtained in three of the five events were satisfactory: the Nash-Sutcliffe coefficient (NSE) oscillated between 0.39 and 0.77, and R^2 oscillated between 0.51 and 0.86. We concluded that the integration of an hourly hydrologic model with IMERG-L satellite rainfall images is a good option in areas where hourly rainfall data measured on land is scarce or non-existent.

Keywords: IMERG satellite rainfall images, Clark's modified unitary hydrogram, HEC-HMS, runoff curve number, Nash-Sutcliffe efficiency (NSE).

INTRODUCTION

Precipitation is a component of the water cycle and a key input of hydrological models (Jiang and Bauer-Gottwein, 2019). In the analysis of extreme events in real time, floods and droughts, it is necessary to have spatially and temporally reliable quantification of rainfall (Zubieta *et al.*, 2018). However, hourly rainfall data measured on land are scarce and even non-existent because of the limited spatial coverage of automatic meteorological stations (AMSs). Moreover, AMSs often fail when registering maximum rainfall. This problem is a challenge for hydrologists when modeling a basin hydrologically. The reliability of modeling results is dependent on the availability of reliable hydrometeorological data for calibrating and validating the model. (Magaña-Hernández *et al.*, 2013).

Over the last two decades, satellite-based rainfall products with broad spatial coverage and high temporal resolution have provided a potential solution to the scarcity of

hourly data measured on land (Bui *et al.*, 2019). Among these satellite-based rainfall products are data from the Global Precipitation Measurement (GPM) mission and the Integrated Multi-satellitE Retrievals for GPM (IMERG). This mission was launched by the National Aeronautics and Space Administration (NASA) and the Japan Aerospace Exploration Agency (JAXA) on February 28, 2014, as the successor of the Tropical Rainfall Measuring Mission (TRMM) to provide near-real-time observations of rain and snowfall. The IMERG version 6 satellite rainfall images (early, late and final execution, IMERG-E, IMERG-L, and IMERG-F) are available 4, 12 h and 3.5 months after the observation, respectively, with a spatial coverage of 0.1 x 0.1° at the global level and a temporal resolution of 30 minutes (Tan *et al.*, 2019).

The integration of satellite-based rainfall products with distributed hydrological models is an option for simulating hydrological processes (Mei *et al.*, 2016). A distributed hydrological model divides the basin into micro-basins or cells to account for spatial variability of the physical properties and rainfall. It also allows for the analysis of the impact of different elements, such as vegetation and land use, on the hydrological response. Moreover, the distributed model allows determining the flow at any point within the basin since it explicitly considers the spatial variation of rainfall, infiltration, losses, and runoff (Méndez-Antonio *et al.*, 2014). Among the different programs for constructing a distributed hydrologic model, the Hydrologic Modeling System (HEC-HMS) developed by the Hydrological Engineering Center of the US Army Corps of Engineers is a program designed to simulate rainfall-runoff and flow transit processes (USACE, 2000).Espinosa-López *et al.* (2020) used IMERG-L, version 5, satellite images in hourly modeling with the HEC-HMS program in the Huaynamota River Basin in Mexico, for three hydrometeorological events covering an area of 12 080 km^2. These authors obtained a maximum Nash-Sutcliffe (NSE) coefficient of 0.531 in the model calibration. They came to the conclusion that hydrologic modeling using IMERG-L satellite rainfall images is a good option in areas where hourly rainfall data measured on land are scarce.

This study had the objective of simulating and calibrating the flows of the Coahuayana River Basin in Jalisco, Mexico, from IMERG-L satellite rainfall images by using the method runoff curve number and Clark's modified unitary hydrogram, with the HEC-HMS program for events of maximum rainfall that occurred in 2010, 2011, 2013, 2015, and 2021.

MATERIALS AND METHODS

Study zone

The Coahuayana River Basin, which is part of the hydrological region 16 Armería-Coahuayana, has an area of 7332 km^2 up to the CONAGUA Callejones hydrometric station and includes parts of the states of Jalisco, Colima, and Michoacán. It is located between 103° 48′ and 102° 55′ W, 20° 1′ and 18° 39′ N (Figure 1). The basin was delimited using a digital elevation model with a resolution of 15 m and ArcGis HEC-

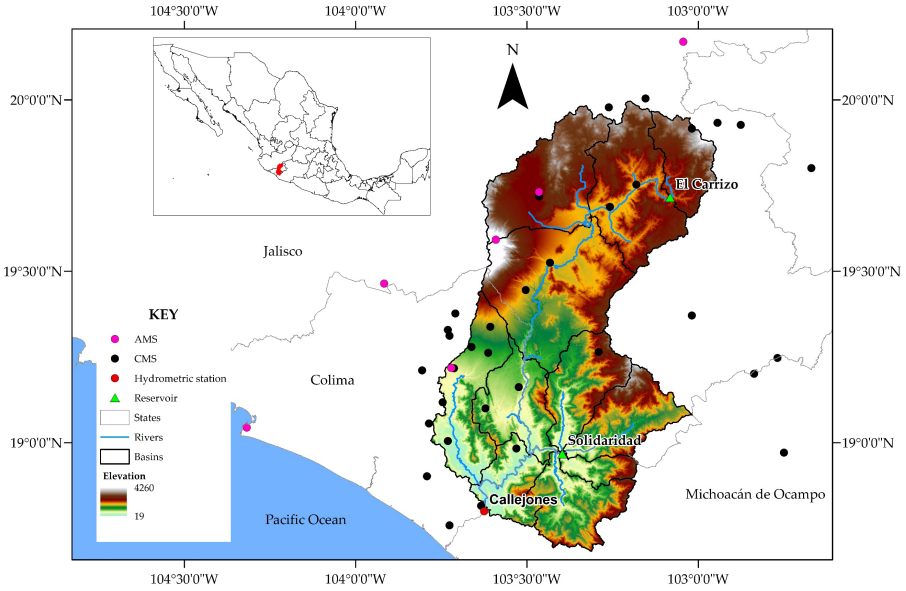

Figure 1. Location of the Coahuayana Basin and the hydrometeorological stations in Jalisco, Mexico.

GeoHMS 10.3. Altitudes range from 16 to 4260 m; the basin has an average slope of 31.6 %, a main channel slope of 0.97 %, and a concentration time of 28 h. The average annual rainfall is 940.72 mm, and the average temperature is 20.74 °C (SMN, 2021c). The basin contributes runoff to the Solidaridad reservoir, which has a capacity of 220 hm^3, and the El Carrizo reservoir, with a 47.27 hm^3 capacity (CONAGUA, 2021). These reservoirs are 30 and 116 km, respectively, upstream from the Callejones gauging station.

Sources of information

The IMERG Late (IMERG-L) version 6 satellite rainfall images have a temporal resolution of 30 min and a spatial resolution of 0.1 x 0.1°. The IMERG-L satellite rainfall images are available for free 12 h after the observation at the web site Global Precipitation Measurement (https://gpm.nasa.gov/data/directory). These images cover a band of 60° S, 60° N for the period from June 2000 to the present (Huffman *et al.*, 2020). They were downloaded in raster format using the FileZilla program and the address jsimpsonftps.pps.eosdis.nasa.gov. To convert universal time (UTC) to local time in the study zone, 5 h were subtracted from the satellite image time.

Precipitation data were collected from conventional meteorological stations (CMS) (SMN, 2021a) and automatic meteorological stations (AMS) (SMN, 2021b), both of which belong to the *Servicio Meteorológico Nacional* (SMN). The 7332 km^2 basin and the distribution of the four AMS and 28 CMS used to calibrate on land are shown (Figure

1). The observed flow data at the Callejones station were obtained from the national databank of surface water (BANDAS) (CONAGUA, 2021).

Information on the storms selected to simulate flows in the Coahuayana River Basin is presented (Table 1). To generate the raster of the runoff curve number (CN), the edaphological vectorial data set was used, scale 1:250 000 series II (INEGI, 2021b), and the vectorial data set on land use and vegetation, scale 1:250 000 series VI (INEGI, 2021a).

Table 1. Modeled hydrometeorological events in the Coahuayana River Basin in Jalisco, Mexico.

Year of the storm	Duration	Average rainfall (mm)	Maximum Flow observed at Callejones (m^3 s^{-1})
2010	July 19 to 31	142	398
2011	October 9 to 19	87	2600
2013	September 13 to 20	116	690
2015	October 20 to 30	157	845
2021	August 20 to 27	64	237

Hydrologic modeling

Hydrologic simulations were carried out in HEC-HMS 4.8 using the method runoff curve number (CN) of the US Soil Conservation Service (SCS) to convert total precipitation over an area into runoff depth. The modeling time interval was 1 h. Merino-Jiménez *et al.* (2021) mention that an hourly hydrological model is constructed as a predictive tool to protect the population and provide more precise information about when the maximum flow will occur. Its construction is important in basins where the concentration time is less than 24 h, and in general, a calibrated hourly model would help decision-making.

The curve number method was developed by the US Department of Agriculture (USDA) of the SCS and is documented in detail in the National Engineering Handbook (Mockus, 2004). In this handbook, the runoff depth for a given rainfall event is calculated as follows:

$$Q = \frac{(P - I_a)^2}{(P - I_a) + S} \quad (1)$$

where Q is the depth of runoff (mm), P is the precipitated depth (mm), S is the maximum potential retention (mm), and I_a is the initial abstraction (mm).

From experimental data on basins, an empirical relationship was found between S and I_a:

$$I_a - 0.2S \quad (2)$$

By substituting Equation (2) in Equation (1), we obtain:

$$Q = \frac{(P - 0.2S)^2}{(P + 0.8S)}$$

where $P > I_a$, otherwise $Q = 0$.

Moreover, the curve number (CN) and maximum potential retention (S), in mm, are related by:

$$S = \frac{25400}{CN} - 254$$

According to the USDA (1986), variability in the curve number is due to the type of cover, soil hydrological group (A, B, C, or D), and previous moisture condition. The last factor is divided into three groups: dry (I), average (II), and moist (III) (Mockus, 2004).
Depending on the depth of rain accumulated five days before the storm, the curve number was corrected in the following manner: if rainfall is less than 25 mm, correction A; if rainfall is more than 25 mm and less than 50 mm, no correction; if rainfall is more than 50 mm, correction B (Aparicio-Mijares, 2001). The rain accumulated five days before the storm was calculated with rainfall information from the conventional and automatic meteorological stations.

Corrections A and B were carried out following Chow *et al.* (1994):

Correction $A = \frac{4.2\,CN}{10 - 0.058\,CN}$

Correction $B = \frac{23\,CN}{10 + 0.13\,CN}$

where *CN* is the curve number in the average antecedent moisture condition obtained from the USDA (1986).

Runoff transfer was calculated with Clark's modified unitary hydrogram method, or ModClark (Yang *et al.*, 1990). The method involves transferring the runoff produced in each cell to the outlet of the basin after a time interval equal to the travel time from the cell to the outlet. The transit time for each cell is calculated with the following equation:

$$t_{cell} = T_c\left(\frac{d_{cell}}{d_{\max}}\right)$$

where t_{cell} is the transit time of the cell (h), d_{cell} is the distance from the cell to the basin outlet (m), d_{max} is the distance from the farthest cell to the outlet (m), and T_c is the basin concentration time (h).

The ModClark method requires estimation of two parameters to calculate the hydrogram produced in the basin: concentration time (T_c) and the storage coefficient (R). Concentration time is defined as the time needed for a drop of water to travel from the farthest point of the basin to the outlet point. T_c was estimated with the Kirpich equation as follows (Karamouz *et al*., 2013):

$$T_c = 0.00325 \frac{L^{0.77}}{S^{0.385}}$$

where T_c is the concentration time (h), L is the length of the main channel (m), and S is the slope of the main channel (m m^{-1}).

The storage coefficient (R) can be estimated by dividing the volume under the hydrogram after the second inflection point (recession curve) by the flow value at this point (USACE, 1982). This coefficient can be estimated using the following equation:

$$R = \frac{\int_{PI}^{\infty} Q(t)}{Q_{PI}} dt$$

where R is the storage coefficient, $\int_{PI}^{\infty} Q(t)$ is the volume under the hydrogram after the second inflection point, and Q_{PI} is the value of the flow at the inflection point. For practical purposes, according to Domínguez-Mora *et al.* (2008), the storage coefficient can be estimated as $R = 0.6\ T_c$. In this study, the value of R for each sub-basin was estimated to be $0.6\ T_c$, which generated the best fit during the process of calibration.

The transit of runoff toward the basin outlet was determined with the method of Muskingum (Karamouz *et al*., 2013), where the output hydrogram in the lower part of the river is calculated for a given entry hydrogram in the upper part of the river:

$$S = K\,[XI + (1 - X)\,Q]$$

where S is the storage in the section, I is the entry flow, Q is the output flow; K is the transit time constant, and X is the weighted factor, which varies between 0 and 1.

According to Aparicio-Mijares (2001), the K parameter can be calculated as the transit time of the wave peak along the entire section:

$$K = \frac{L}{w}$$

where L is the length of the reach (m) and w is the mean speed of the wave (m s^{-1}). w can be calculated as 1.5 times the mean speed of the water in the section, and the latter can be obtained according to the slope of the main channel. Aparicio-Mijares (2001) recommends that, when information is lacking, the value 0.2 be used as the weight factor.

Model entry data

The basin was delimited using ArcGis HEC-GeoHMS 10.3, based on the digital elevation model obtained from the continuum of Mexican elevations 3.0 (CEM 3.0) (INEGI, 2021c) with the Callejones hydrometric station 16 022 at 103° 37′ W and 18° 48′ N as the exit point (CONAGUA, 2021). Using the methodology proposed by the USACE (2013), the following sub-basin characteristics were determined: area, slope, length of the main channel, slope of the main channel, and the HMS hydrological scheme.

The satellite rainfall images were processed in ArcMap 10.3 from ArcGis. The satellite images in raster format with a cell size of 2 x 2 km were transformed into ASCII format and used to generate a *.dss file with the Hec-GeoHMS 10.3 tool asc2dssGrid.exe. This file contains the registers of rain from each satellite image for the relevant storm and was imported into HEC-HMS. To obtain the runoff curve number, a file in raster format was generated with the series II (INEGI, 2021b) set of edaphological vectorial data and the series VI (INEGI, 2021a) set of vectorial data on land use and vegetation, applying the methodology proposed by USACE (2013) in the HEC-GeoHMS 10.3 extension of ArcGis.

Calibration of the hydrologic model in HEC-HMS

Calibration consists of fitting the value of each model parameter so that the hydrogram obtained in the simulation adjusts to the observed hydrogram of the basin. Calibration of the model in HEC-HMS 4.8 was performed with the optimization module included in the software. The Nelder and Mead method (USACE, 2000) was used as the search algorithm for the optimal value of the model parameters. This method uses a simplex algorithm to evaluate all the parameters simultaneously and determine which parameter to adjust. The target function measures the goodness of fit between the calculated and observed hydrograms. We used the objective function root mean square error peak weighted, which gives more weight to flows that are above the mean and less weight to flows that are below the mean.

The optimized parameters were the curve number (CN) and the concentration time (T_c) of each sub-basin, varying their values up to ± 20 %.

Measurement of the hydrologic model fit

To evaluate the hydrologic model fit, three statistical indicators were used: the Nash-Sutcliffe coefficient (NSE) (Nash and Sutcliffe, 1970), the coefficient of determination (R^2), and the root mean square error (RMSE) (Vargas-Castañeda *et al.*, 2015).

Moriasi *et al.* (2015) recommend the following classification for the NSE index and R^2 to evaluate hydrological simulations: very good, $0.75 < NSE \leq 1.00$, $0.85 < R^2 \leq 1.00$; good, $0.65 < NSE \leq 0.75$, $0.75 < R^2 \leq 0.85$; satisfactory, $0.50 < NSE \leq 0.65$, $0.60 < R^2 \leq 0.75$; unsatisfactory, $NSE \leq 0.50$, $R^2 \leq 0.60$. These authors point out that NSE values between 0 and 1 are considered acceptable, while NSE values < 0 indicate that the mean is a better predictor than the simulated value, meaning that the model is inefficient.

It is important to note that the above classification refers to models with a monthly time scale, whereas the model for this study is hourly. For this reason, the classification for hourly models may be less severe because predicting hourly events is more difficult than predicting monthly events.

RESULTS AND DISCUSSION

On data from GPM-IMERG satellite images

In this 7332 km^2 area of the basin, information from 4 AMS and 28 CMS from the SMN were used to calibrate the information obtained from the images. Some CMS and AMS were in the immediate periphery of the ridge of the basin (Figure 1). In this study, the IMERG product with a 30 min temporal resolution was used, available in open form at the web site Global Precipitation Measurement (https://gpm.nasa.gov/data/directory). Hourly and daily rainfall data measured on land were compared to those from IMERG-L (late), which was available 12 hours after the rainfall event. Among the main findings were: (a) the best R^2 for fitting daily and hourly rainfall were 0.83 and 0.42, respectively; (b) the IMERG satellite rainfall images more precisely detect daily precipitations above 20 mm; and (c) IMERG satellite rainfall images have the best fit for pluviometric stations located at low elevations.

The hydrologic model

The Coahuayana Basin, for better precision in its analysis, was divided into eleven sub-basins. The basin has an average slope of 31.6 % and an average runoff curve number of 58. The values for curve number and concentration times obtained in the calibration for each event and their modification relative to the initial value are shown (Tables 2 and 3).

The results of the hydrological models calibrated with satellite rainfall images are shown (Table 4). They show NSE values greater than zero, indicating that the calibrated hydrological model is a better predictor than the mean of the observed flows. According to the classification recommended by Moriasi *et al.* (2015), the hydrological model of the 2010 event has a satisfactory fit, the model of the 2013 event has a good fit, and the model of the 2015 event has a very good fit.

The NSE coefficients of three of the five modeled events are greater than 0.5, indicating that rainfall satellite images can be used for hydrological modeling. It is important to note that the model provides an excellent total runoff depth during the event (L_{mod}) when compared to the observed depth (L_{obs}) (Table 4). The depth of runoff multiplied by the area of the basin is the total runoff volume.

Table 2. Runoff curve number for optimization by sub-basin and event in the Coahuayana River Basin in Jalisco, Mexico.

Year Sub-basin	2010 Mod. (%)ǂ	2011 Mod. (%)	2013 Mod. (%)	2015 Mod. (%)	2021 Mod. (%)
W360	11.1	19.4	19.4	13.0	15.4
W340	5.6	12.9	19.9	12.7	8.9
W330	13.9	14.0	-18.8	20.1	19.7
W320	19.1	20.0	-19.9	19.9	3.4
W500	3.0	19.9	-5.7	20.0	-4.5
W300	-19.9	16.8	-2.1	17.1	-11.2
W290	-12.6	20.0	-2.5	20.0	-13.1
W270	-20.0	19.7	-2.5	19.8	-13.1
W450	-15.6	18.6	1.7	18.8	-9.6
W410	-13.6	19.3	-7.8	18.4	-15.6
W490	-19.8	2.0	-3.0	19.8	-11.8

ǂMod: modification in % of the curve number.

Table 3. Concentration time modified for optimization of each event.

Year Sub-basin	2010 Mod. (%)ǂ	2011 Mod. (%)	2013 Mod. (%)	2015 Mod. (%)	2021 Mod. (%)
W360	-18.7	7.1	-2.9	12.4	-15.9
W340	-14.7	11.8	-16.0	8.7	-14.4
W330	-8.3	7.2	-16.3	8.3	-19.4
W320	-13.7	8.0	-9.3	12.3	-18.3
W500	-11.8	12.7	-4.8	3.2	-9.8
W300	-19.0	8.9	-18.8	-4.6	-8.0
W290	-18.1	-6.1	-9.3	-7.9	-13.2
W270	8.3	3.8	19.9	-12.8	-10.8
W450	5.5	3.9	-4.9	-12.7	-13.3
W410	-19.7	8.9	-18.6	-6.9	-11.1
W490	-4.1	-5.0	2.0	-7.9	-7.0

ǂMod: modification in % of the curve number.

Table 4. Hourly hydrological model results calibrated for the Coahuayana River Basin in Jalisco, Mexico.

Storm	Q_{obs} ($m^3 s^{-1}$)	Q_{mod} ($m^3 s^{-1}$)	L_{obs} (mm)	L_{mod} (mm)	NSE	R^2	RMSE ($m^3 s^{-1}$)
2010	398	328	16.4	19.5	0.61	0.68	59
2011	2600	841	40.0	34.6	0.39	0.61	532
2013	690	651	22.9	20.9	0.73	0.79	89
2015	845	774	26.1	18.2	0.77	0.86	107
2021	237	261	10.5	10.6	0.49	0.51	29

Q: flows; L: runoff depth; obs: observed; mod: modeled. Statistical indicators NSE: Nash-Sutcliffe coefficient; R^2: determination coefficient; RSME: mean error root square.

Results show that there is no relationship between the model fit and the maximum observed flow. A positive relationship between the NSE coefficient and the maximum observed flow is observed in the events of 2021 (0.49, 236.8 $m^3 s^{-1}$), 2010 (0.61, 398.3 $m^3 s^{-1}$), 2013 (0.73, 690 $m^3 s^{-1}$), and 2015 (0.77, 845 $m^3 s^{-1}$). However, the 2011 event (0.39, 2600 $m^3 s^{-1}$) contradicts this trend. Although the 2011 event had an NSE of 0.39, its R^2 (0.61) was higher than that obtained in the 2021 event (0.51), with an NSE of 0.49.

The maximum modeled flows underestimated the maximum observed flows in the events of 2010, 2011, 2013, and 2015 (Table 4). Although the 2011 event had an NSE of 0.39, the difference between runoff depths or volumes (13.3 %) was lower than the difference obtained in the 2015 event (30.4 %) with an NSE of 0.77. The 2013 event had a smaller difference between flows, 5.7 % lower and 5 h after the maximum observed flow.

The dynamics and magnitude of the modeled and observed flows of the 2010 event are shown (Figure 2); it can be observed that the model overestimated the flows between July 28 and 30. For this reason, the model achieved an NSE of 0.61. From the dynamics and magnitude of the modeled and observed flows of the 2015 event (Figure 3), the model underestimated the flows between October 27 and 30, and for this reason, it achieved an NSE of 0.77. Meanwhile, from the dynamics and magnitude of the modeled and observed flows of the 2021 event (Figure 4), the model overestimated the flows between August 25 and 27, and achieved an NSE of 0.49.

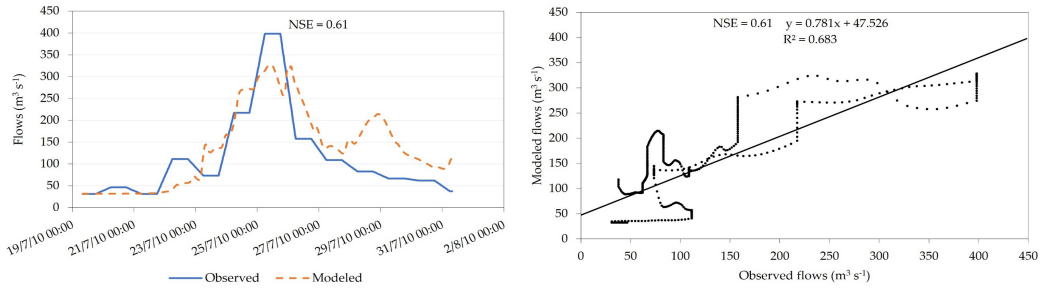

Figure 2. Hydrogram of the Callejones station in the event of July 19 to 31, 2010.

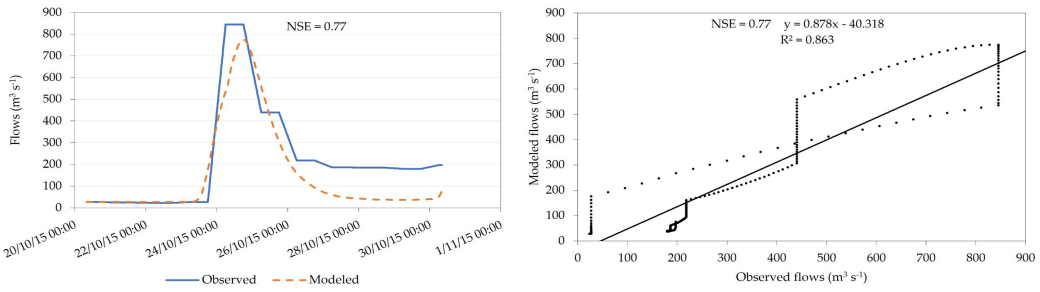

Figure 3. Hydrogram of the Callejones station during the event of October 20 to 30, 2015.

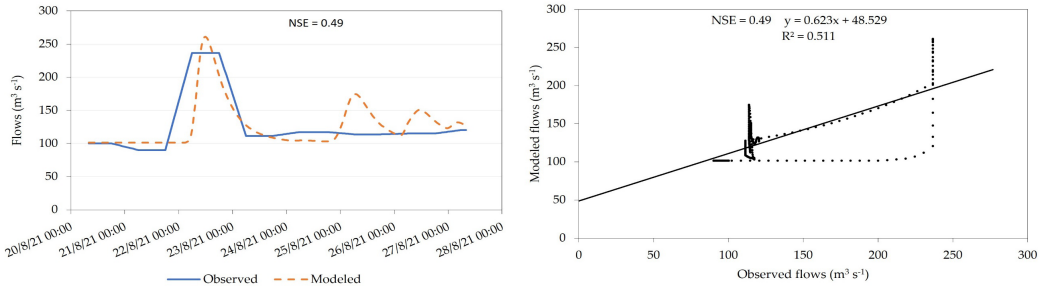

Figure 4. Hydrogram of the Callejones station during the event of August 20 to 27, 2021.

The NSE value of 0.77 obtained in this study, when compared with the 0.531 of the hourly hydrologic model of Espinosa-López *et al.* (2020) for the Huaynamota River Basin in Nayarit, had better results. The duration of the two events was 10 days, with a maximum observed flow of 845 and 465.9 $m^3 s^{-1}$ for this and the other study, respectively. The basins have areas of 7332 km^2 and 12 080 km^2, respectively, and thus, the size of the basin presents a challenge for spatial distribution of the precipitation.

CONCLUSIONS

The distributed hydrologic models obtained at the Coahuayana River Basin outlet from IMERG-L satellite rainfall images and the program HEC-HMS, based on the curve number method to calculate losses and Clark's modified unitary hydrogram for the hydrograms were satisfactory, according to the Nash-Sutcliffe coefficients, during the maximum precipitation events in July 2010, September 2013, and October 2015.

Because precipitation provides important entry data in hydrologic modeling, calibrating the IMERG-L satellite rainfall images using hourly rainfall data measured on land is recommended. The improved results of this study, when compared to previous work, demonstrate how the quality of GPM-IMERG-L satellite rainfall images has improved in contrast to real measurements on land. From the results obtained by hourly modeling, it is concluded that the IMERG-L satellite rainfall images are a good option as entry data in distributed hydrologic modeling in places where hourly rainfall data measured on land are scarce or non-existent.

ACKNOWLEDGEMENTS

The authors would like to thank the *Consejo Nacional de Ciencia y Tecnología* (CONACYT) for the two-year national grant and the *Servicio Meteorológico Nacional* for the hourly rainfall data provided through direct communication.

REFERENCES

Aparicio-Mijares FJ. 1992. Fundamentos de hidrología de superficie. Limusa: Ciudad de México, México. 303 p.

Bui HT, Ishidaira H, Shaowei N. 2019. Evaluation of the use of global satellite–gauge and satellite-only precipitation products in stream flow simulations. Applied Water Science 9 (3): 1–15. https://doi.org/10.1007/s13201-019-0931-y

Chow VT, Maidment DR, Mays LW. 1994. Hidrología Aplicada. McGraw Hill: Bogotá, Colombia. 584 p.

CONAGUA (Comisión Nacional del Agua). 2021. Banco nacional de datos de aguas superficiales. Comisión Nacional del Agua. Ciudad de México, México. https://sih.conagua.gob.mx/ (Retrieved: November 2021).

Domínguez-Mora R, Esquivel-Garduño G, Baldemar-Méndez A, Mendoza-Reséndiz A, Arganis-Juárez ML, Carrizosa-Elizondo E. 2008. Manual del modelo para prónostico de escurrimiento. Instituto de Ingeniería. Universidad Nacional Autónoma de México: Ciudad de México, México. https://doi.org/10.13140/RG.2.1.4687.5287

Espinosa-López JA, Ibáñez-Castillo LA, Arteaga-Ramírez RA, Galeana-Pizaña JM. 2020. Modelo hidrológico distribuido con imágenes GPM-IMERG en la cuenca del río Huaynamota, Nayarit, México. Tecnologia y Ciencias del Agua 11 (5): 344–383. https://doi.org/10.24850/j-tyca-2020-05-09

Huffman GJ, Bolvin DT, Braithwaite D, Hsu K, Joyce R, Kidd C, Nelkin EJ, Sorooshian S, Tan J, Xie P. 2020. NASA Global Precipitation Measurement (GPM) Integrated Multi-satellitE Retrievals for GPM (IMERG). Algorithm Theoretical Basis Document (ATBD), Version 6. National Aeronautics and Space Administration: Greenbelt, MD, USA. https://pmm.nasa.gov/sites/default/files/document_files/IMERG_ATBD_V06.pdf (Retrieved: November 2021).

INEGI (Instituto Nacional de Estadística y Geografía). 2021a. Conjunto de datos vectoriales de uso del suelo y vegetación serie VI. Instituto Nacional de Estadística y Geografía. Ciudad de México, México. https://www.inegi.org.mx/temas/usosuelo/#Descargas (Retrieved: November 2021).

INEGI (Instituto Nacional de Estadística y Geografía). 2021b. Conjunto de datos vectoriales edafológicos serie II. Instituto Nacional de Estadística y Geografía. Ciudad de México, México. https://www.inegi.org.mx/temas/edafologia/#Descargas (Retrieved: November 2021).

INEGI (Instituto Nacional de Estadística y Geografía). 2021c. Continuo de elevaciones mexicano 3.0. Instituto Nacional de Estadística y Geografía. Ciudad de México, México. https://www.inegi.org.mx/app/geo2/elevacionesmex/ (Retrieved: November 2021).

Jiang L, Bauer-Gottwein P. 2019. How do GPM IMERG precipitation estimates perform as hydrological model forcing? Evaluation for 300 catchments across Mainland China. Journal of Hydrology 572: 486–500. https://doi.org/10.1016/j.jhydrol.2019.03.042

Karamouz M, Nazif S, Falahi M. 2013. Hydrology and hydroclimatology: principles and applications. CRC Press: Boca Raton, FL, USA.

Magaña-Hernández F, Bâ KM, Guerra-Cobián VH. 2013. Estimación del hidrograma de crecientes con modelación determinística y precipitación derivada de radar. Agrociencia 47 (8): 739–752.

Mei Y, Nikolopoulos EI, Anagnostou EN, Borga M. 2016. Evaluating satellite precipitation error propagation in runoff simulations of mountainous basins. Journal of Hydrometeorology 17 (5): 1407–1423. https://doi.org/10.1175/JHM-D-15-0081.1

Méndez-Antonio B, Soto-Cortés G, Rivera-Trejo F, Caetano E. 2014. Modelación hidrológica distribuida apoyada en radares meteorológicos. Tecnología y Ciencias del Agua 5 (1): 83–101. https://www.scielo.org.mx/scielo.php?script=sci_arttext&pid=S2007-24222014000100006

Merino-Jiménez E, Ibáñez-Castillo LA, Arteaga-Ramírez R, Vázquez-Peña MA. 2021. Hourly hydrologic modeling in the upper basin of the Fuerte River, Sinaloa, Mexico. Ingeniería Agrícola y Biosistemas 13 (1): 53–76. https://doi.org/10.5154/r.inagbi.2020.11.085

Mockus V. 2004. National engineering handbook, section 4: hydrology. Soil Conservation Service: Washington, DC, USA. 127 p.

Moriasi DN, Gitau MW, Pai N, Daggupati P. 2015. Hydrologic and water quality models: Performance measures and evaluation criteria. American Society of Agricultural and Biological Engineers 58 (6): 1763–1785. https://doi.org/10.13031/trans.58.10715

Nash JE, Sutcliffe J V. 1970. River flow forecasting through conceptual models part I - a discussion of principles. Journal of Hydrology 10: 282–290. https://doi.org/10.1016/0022-1694(70)90255-6

SMN (Servicio Meteorológico Nacional). 2021a. Información estadística climatológica. Servicio Meteorológico Nacional. Ciudad de México, México. https://smn.conagua.gob.mx/es/climatologia/informacion-climatologica/informacion-estadistica-climatologica (Retrieved: November 2021).

SMN (Servicio Meteorológico Nacional). 2021b. Información meteorológica. Servicio Meteorológico Nacional. Ciudad de México, México. https://smn.conagua.gob.mx/es/observando-el-tiempo/estaciones-meteorologicas-automaticas-ema-s (Retrieved: November 2021).

SMN (Servicio Meteorológico Nacional). 2021c. Sistema clima computarizado (CLICOM). Servicio Meteorológico Nacional. Ciudad de México, México. http://clicom-mex.cicese.mx/malla/index.php (Retrieved: November 2021).

Tan J, Huffman GJ, Bolvin DT, Nelkin EJ. 2019. IMERG V06: Changes to the morphing algorithm. Journal of Atmospheric and Oceanic Technology 36 (12): 2471–2482. https://doi.org/10.1175/JTECH-D-19-0114.1

USACE (United States Army Corps of Engineers). 1982. Hydrologic Analysis of Ungaged Watershed Using HEC-1. United States Army Corps of Engineers. Hydrologic Engineering Center. Davis, CA, USA. https://www.hec.usace.army.mil/publications/TrainingDocuments/TD-15.pdf (Retrieved: November 2021).

USACE (United States Army Corps of Engineers). 2000. Hydrologic Modeling System HEC-HMS Technical Reference Manual. United States Army Corps of Engineers. Hydrologic Engineering Center. Davis, CA, USA. https://www.hec.usace.army.mil/software/hec-hms/documentation/HEC-HMS_Technical Reference Manual_(CPD-74B).pdf (Retrieved: November 2021).

USACE (United States Army Corps of Engineers). 2013. HEC-GeoHMS geospatial hydrologic modeling extension: User's Manual Version 10.1. United States Army Corps of Engineers. Hydrologic Engineering Center. Davis, CA, USA. https://www.hec.usace.army.mil/software/hec-geohms/documentation/HEC-GeoHMS_Users_Manual_10.1.pdf (Retrieved: November 2021).

USDA (United States Department of Agriculture). 1986. Urban hydrology for small wathersheds TR-55. United States Department of Agriculture. Washington, DC, USA. https://www.nrcs.usda.gov/Internet/FSE_DOCUMENTS/stelprdb1044171.pdf (Retrieved: November 2021).

Vargas-Castañeda G, Ibáñez-Castillo LA, Arteaga-Ramírez R. 2015. Development, classification and trends in rainfall-runoff modeling. Ingeniería Agrícola y Biosistemas 7 (1): 5–21. https://doi.org/10.5154/r.inagbi.2015.03.002

Yang MS, Kull DW, Feldman AD. 1999. Evolution of Clark's Unit Graph Method to spatially distributed runoff. Journal of Hydrologic Engineering 3 (1): 9–19. https://doi.org/10.1061/(asce)1084-0699(1999)4:1(89)

Zubieta R, Laqui W, Lavado W. 2018. Modelación hidrológica de la cuenca del río Ilave a partir de datos de precipitación observada y de satélite, periodo 2011-2015, Puno, Perú. Tecnologia y Ciencias del Agua 9 (5): 85–105. https://doi.org/10.24850/j-tyca-2018-05-04